CellPress

Remodeling of Channel-Forming ORAI Proteins Determines an Oncogenic Switch in Prostate Cancer

Charlotte Dubois,[1,4] Fabien Vanden Abeele,[1,4,5,*] V'yacheslav Lehen'kyi,[1] Dimitra Gkika,[1] Basma Guarmit,[3] Gilbert Lepage,[1] Christian Slomianny,[1] Anne Sophie Borowiec,[1] Gabriel Bidaux,[1] Mohamed Benahmed,[3] Yaroslav Shuba,[1,2] and Natalia Prevarskaya[1,5,*]

[1]Inserm U1003, Laboratory of Excellence, Ion Channels Science and Therapeutics, Equipe Labellisée par la Ligue Nationale Contre le Cancer, SIRIC ONCOLille, Université des Sciences et Technologies de Lille, Villeneuve d'Ascq 59656, France

[2]Bogomoletz Institute of Physiology and International Centre of Molecular Physiology of the National Academy of Sciences of Ukraine, Kiev 01024, Ukraine

[3]Inserm, INSERM U895, Centre Méditerranéen de Médecine Moléculaire, Hôpital l'Archet, Nice 06202, France

[4]Co-first author

[5]Co-senior author

*Correspondence: Fabien.vanden-abeele@inserm.fr (F.V.A.), natacha.prevarskaya@univ-lille1.fr (N.P.)

http://dx.doi.org/10.1016/j.ccr.2014.04.025

SUMMARY

ORAI family channels have emerged as important players in malignant transformation, yet the way in which they reprogram cancer cells remains elusive. Here we show that the relative expression levels of ORAI proteins in prostate cancer are different from that in noncancerous tissue. By mimicking ORAI protein remodeling observed in primary tumors, we demonstrate in in vitro models that enhanced ORAI3 expression favors heteromerization with ORAI1 to form a novel channel. These channels support store-independent Ca^{2+} entry, thereby promoting cell proliferation and a smaller number of functional homomeric ORAI1-based store-operated channels, which are important in supporting susceptibility to apoptosis. Thus, our findings highlight disrupted dynamic equilibrium of channel-forming proteins as an oncogenic mechanism.

INTRODUCTION

Calcium is a universal messenger regulating many physiological functions including cell proliferation and apoptosis, two key processes determining normal tissue homeostasis. We and others have shown that calcium homeostasis is disrupted during carcinogenesis, thereby leading to deregulated cell proliferation and suppression of apoptosis (for reviews see Monteith et al., 2007; Roderick and Cook, 2008; Prevarskaya et al., 2011).

A number of studies have demonstrated that a large, sustained elevation of the concentration of cytosolic Ca^{2+} ($[Ca^{2+}]_c$), which is required for triggering apoptosis in cancer cells, is mainly provided by store-operated calcium entry (SOCE), mediated by store-operated channels (SOCs) (Vanden Abeele et al., 2002; Flourakis et al., 2010; Orrenius et al., 2003). SOCs are located in the plasma membrane (PM) and are activated by the depletion of the endoplasmic reticulum (ER) Ca^{2+} store, in response to the stimulation of surface receptor-coupled signaling pathways or ER stress-inducing insults. Molecular players and events resulting in SOCE became increasingly clear when one considers the involvement of two key proteins, STIM1 and ORAI1 (Berna-Erro et al., 2012a). The first of these acts in the ER membrane as a $[Ca^{2+}]_{ER}$ sensor, and the second represents a channel-forming subunit of PM Ca^{2+}-permeable store-operated channel (SOC), which can be activated upon interaction with STIM1 (Zhang et al., 2006; Peinelt et al., 2006; Soboloff et al., 2006; Mercer et al., 2006). Both proteins are members of homologous protein families that include two STIM isoforms, STIM1 and STIM2 (corresponding to *STIM1* and *STIM2* human genes), and three ORAI isoforms, ORAI1, ORAI2, and ORAI3 (corresponding to

Significance

Normal cell progression to their malignant derivatives is associated with remodeling of the proteins controlling such major cellular functions as apoptosis and proliferation. Here, we show that prostate cancer cells use ORAI protein redistribution as an oncogenic switch mechanism. In particular, ORAI3 remodeling results from genomic and microenvironment perturbations that disrupt the equilibrium of ORAI channels and favors the formation of store-independent Ca^{2+} channels activated by arachidonic acid. This remodeling of Ca^{2+} signaling in turn induces cell progression to a more aggressive pro-proliferative phenotype. Our study specifically positions these channels at the center of molecular machinery linking dysregulated arachidonic acid metabolism, calcium homeostasis, and oncogenesis.

the *ORAI1*, *ORAI2*, and *ORAI3* human genes) (Williams et al., 2001; Feske et al., 2006).

Characterization of the molecular nature of SOCE has allowed its general significance to be assessed, as well as that of each of its components in those processes determining malignant growth, such as proliferation, apoptosis, and migration (Faouzi et al., 2011; Motiani et al., 2010; Feng et al., 2010; Yang et al., 2009; Chen et al., 2013; Berna-Erro et al., 2012b). It has been shown that the "classical" interaction of STIM1 and ORAI1 underlies SOCE both in native cancer cells from different types of tumors and in cancer-derived cell lines. At the same time, a number of important "nonclassical" events involving other members of STIM and ORAI families, as well as some nonrelated proteins, have been reported. For example, ORAI1 in human breast cancer (HBC) cells is able to interact with the secretory pathway Ca^{2+}-ATPase to elicit constitutive store-independent Ca^{2+} entry, hence promoting tumorigenesis (Feng et al., 2010). In HBC cells, the molecular composition of SOCE was shown to depend on the estrogen receptor status shifting from a canonical ORAI1 configuration in the estrogen receptor-negative cells to an ORAI3-based one in the estrogen receptor-positive cells, thereby conferring apoptosis resistance (Motiani et al., 2010, 2013; Faouzi et al., 2011). These data clearly show that ORAI proteins are involved in the complex machinery of carcinogenesis; however, the role of their remodeling in the alteration of calcium entry pathways promoting the switch to a more aggressive oncogenic cell phenotype still remains poorly characterized and poses a number of important questions: (1) What is the critical factor for the observed oncogenic switch: the change in the expression level of an individual protein or the change in the ratio of different channel-forming proteins? (2) Does the pathway of calcium entry (for instance agonist-operated versus store-operated) determine a cell's future phenotype? (3) What is the role of ORAI proteins in cancer progression? In particular, the role of ORAI3 needs to be delineated, because this protein is quite exceptional in that it can form both store-dependent and store-independent Ca^{2+} entry channels (Shuttleworth, 2012; González-Cobos et al., 2013). Here we investigated a role for ORAI proteins as calcium signaling gatekeepers in the cancer hallmarks of enhanced growth and resistance to apoptosis.

RESULTS

ORAI3 Is Overexpressed in Human PCa Compared with Healthy Tissues

Before investigating the role of specific ORAI isoforms and STIM1 in the cancer-related processes of human prostate, we first compared their mRNA expression in noncancerous and cancer prostate tissue specimens obtained from resection surgeries. As shown in Figure 1A, only the mRNA for ORAI3 was strongly overexpressed.

ORAI1 and STIM1 Are SOCE Constituents in PCa Cells

We next used patch-clamp and Ca^{2+} imaging techniques combined with small interference (siRNA)-mediated knockdown in order to determine the preferred molecular organization of SOCE in PCa cells. Store-operated current (I_{SOC}) in LNCaP cells was activated in patch-clamp experiments by the intracellular dialysis of a BAPTA-rich (10 mM) pipette solution (Figures 1B and 1C). A 48 hr treatment of the cells with specific siRNAs produced a strong reduction in both mRNA (Figure S1A) and protein expression (Figure S1B), although the impact on I_{SOC} density was variable. Figures 1D and 1E show that only ORAI1 or STIM1 knockdown was correlated with any substantial suppression of I_{SOC} density. We confirmed this result using an intracellular Ca^{2+} imaging technique and the SERCA pump inhibitor thapsigargin (TG) as a store-depleting agent. As expected, the addition of 2 mM extracellular calcium to LNCaP cells, preincubated for 10 min with TG (1 μM) in Ca^{2+}-free medium to achieve complete depletion of their ER Ca^{2+} stores, resulted in the marked and sustained elevation of $[Ca^{2+}]_c$ caused by the activation of SOCE (Figure 1F). The peak $[Ca^{2+}]_c$ elevation, in relation to SOCE, decreased by approximately 60% and 80% in LNCaP cells transfected with siRNA against ORAI1 (siORAI1) or STIM1, respectively, but not with siRNA against other ORAI members (Figures 1F and 1G). Moreover, similar calcium imaging experiments conducted on androgen-independent PCa cells, LNCaP C4-2 (Figure S1C available online), PC-3 (Figure S1D), and DU-145 (Figure S1E), showed that only specific siRNA-mediated knockdown of either ORAI1 or STIM1 impairs their TG-dependent Ca^{2+} entry.

ORAI, but Not STIM1 Isoforms Influence PCa Cell Proliferation

We next examined how siRNA-mediated silencing affects the growth of LNCaP cells. In this series of experiments, cells were transfected with specific anti-STIM1 or anti-ORAI siRNA, and growth was quantified 7 days after transfection. The number of viable proliferating cells was measured by 3-(4,5-dimethylthiazol-2-yl)-5-(3-carboxymethoxyphenyl)-2-(4-sulfophenyl)-2H-tetrazolium (inner salt) assay and manual counting of viable proliferating cells (Figures 2A and 2B). siRNA-mediated knockdown of any of the ORAI or STIM isoforms in LNCaP cells did not affect mitochondrial deshydrogenase (NADH dehydrogenase) activity (Figure S2A), indicating the preservation of bioenergetic status of the cells. At the same time, silencing of any of the ORAI proteins substantially reduced LNCaP proliferation (Figures 2A and 2B), whereas silencing of STIM1 was without any effect. Similar results were obtained with LNCaP C4-2, PC-3, and DU-145 cells (Figures S2B–S2D). The impairment of cell proliferation by ORAI protein knockout, together with the independence of proliferation on the level of STIM1 expression, argues against the involvement of SOCE in these effects. The growth inhibition induced by siRNA against ORAI isoforms was not due to apoptosis (Figure 2C).

Silencing of ORAI Isoforms Mediate a Downregulation of the Oncogenic Cell-Cycle Protein Cyclin D1, which Is Involved in G1 Phase Progression

To elucidate the mechanism by which ORAI proteins influence PCa cell proliferation, we studied the effects of siRNA-mediated silencing of ORAI isoforms on cell-cycle progression using flow cytometry. The results of these experiments have shown that silencing of ORAI1, ORAI2, or ORAI3 in LNCaP cells induced cell-cycle arrest with a significant accumulation of cells in the G0/G1 phase and a decrease in the percentage of the cells in both the S and G2/M phases (Figure 2D). As expected, silencing STIM1 was ineffective on cell-cycle progression (Figure 2D). Similar effects were also observed in PC-3 cells (data not

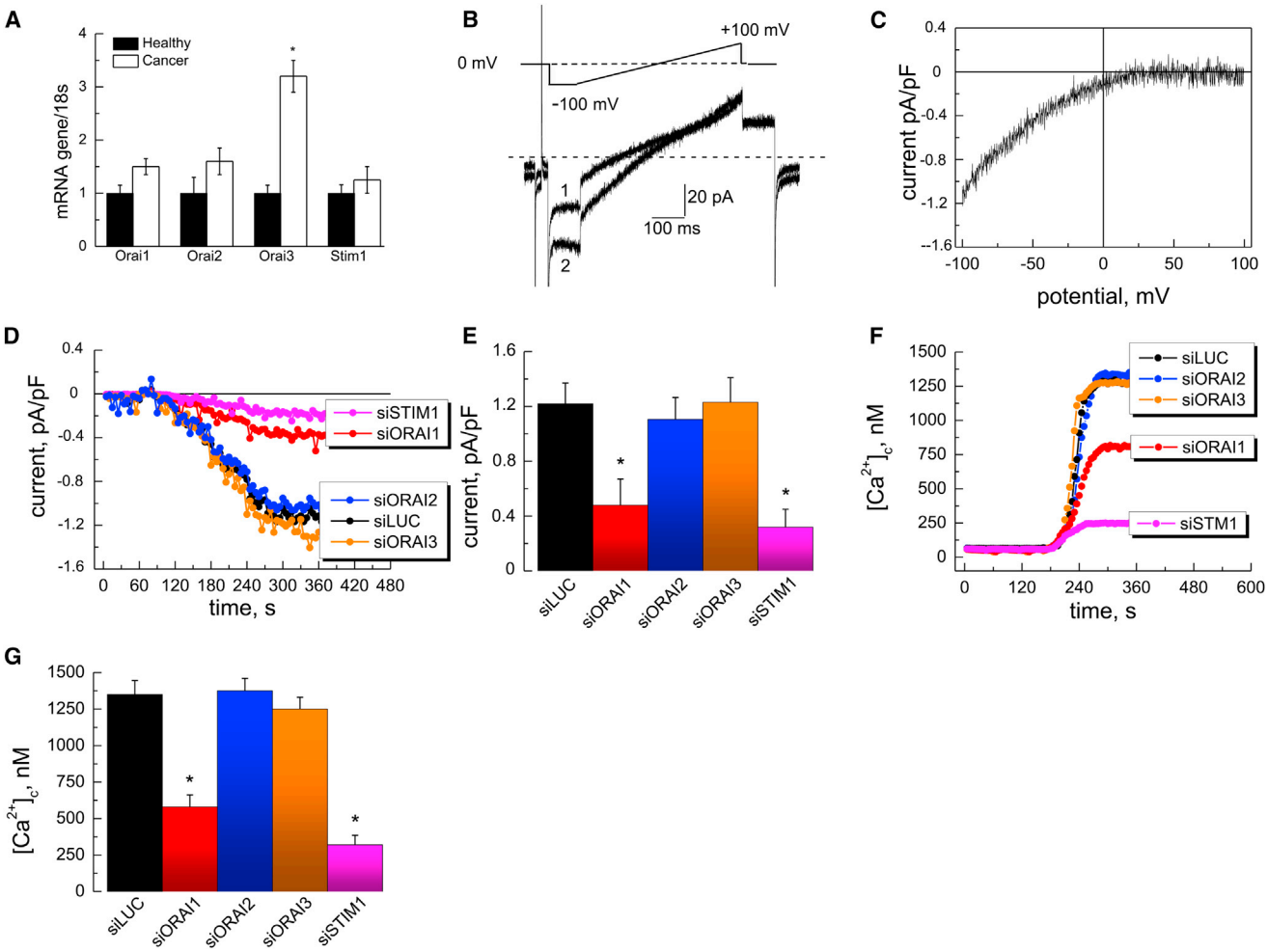

Figure 1. ORAI3 Is Overexpressed in Human PCa Compared to Healthy Tissues but Is Not Involved in SOCE in PCa Cells

(A) PCR quantitation of various ORAI and STIM1 transcripts in PCa compared to healthy tissues.

(B) Traces of base-line current after the rupture of the membrane (1) and fully developed I_{SOC} (2) in representative LNCaP cells, together with the voltage protocol used to elicit the current.

(C) I-V relationship of a fully-developed I_{SOC} derived from the traces presented in (B).

(D) Representative time courses of the development of I_{SOC} in response to dialysis with a 10 mM BAPTA-containing pipette solution in LNCaP cells subjected to 48 hr siRNA-mediated silencing of ORAI isoforms or STIM1 compared to control anti-luciferase siRNA (siLUC); I_{SOC} amplitude was measured at −100 mV.

(E) Quantification of I_{SOC} amplitudes of the results presented in (D) ($n > 10$ for each condition).

(F) Representative measurements of TG-activated SOCE, as indicated by $[Ca^{2+}]_c$ elevation in LNCaP cells 48 hr after treatment with control (siLUC), anti-ORAI isoform-specific, or anti-STIM1 siRNA.

(G) Quantification of SOCE of the results presented in (F) ($n > 50$ for each condition). Data are representative of three independent experiments.

*$p < 0.05$. Error bars represent means ± SEM. See also Figure S1.

shown). Moreover, western blot analysis revealed that an accumulation of LNCaP, DU-145, and PC-3 cells in the G0/G1 phase in response to anti-ORAI treatments was accompanied by a decreased expression of a key controller of G1/S phase transition, cyclin D1 (Figure 2E; Figures S2E and S2F). This would suggest that the influence of ORAIs on proliferation involves an induction of cell-cycle initiator genes.

Downregulation of ORAI Isoforms Alters Both Cytosolic and Endoplasmic Reticulum Calcium Concentration Leading to ER Stress Response

Because, on the one hand, our results indicate that ORAI but not STIM isoforms influence PCa cell proliferation without the involvement of SOCE, but, on the other hand, it is known that calcium signaling is critically important for proliferation (Machaca, 2010), we next asked what other features of calcium homeostasis besides SOCE may be affected by downregulated expression of ORAI proteins. Figure 3A shows original traces obtained from these Ca^{2+} imaging experiments. Resting $[Ca^{2+}]_c$ levels were significantly decreased by siORAI1, siORAI2, or siORAI3 treatments (Figures 3A and 3B). Moreover, the application of the Ca^{2+} ionophore ionomycin (IM, 5 μM), which is able to completely deplete ER Ca^{2+} stores in the Ca^{2+}-free extracellular medium, induced much smaller transient increases in $[Ca^{2+}]_c$ in siRNA-treated LNCaP cells (Figures 3C and 3D), compared with the respective nontreated controls, suggesting that the

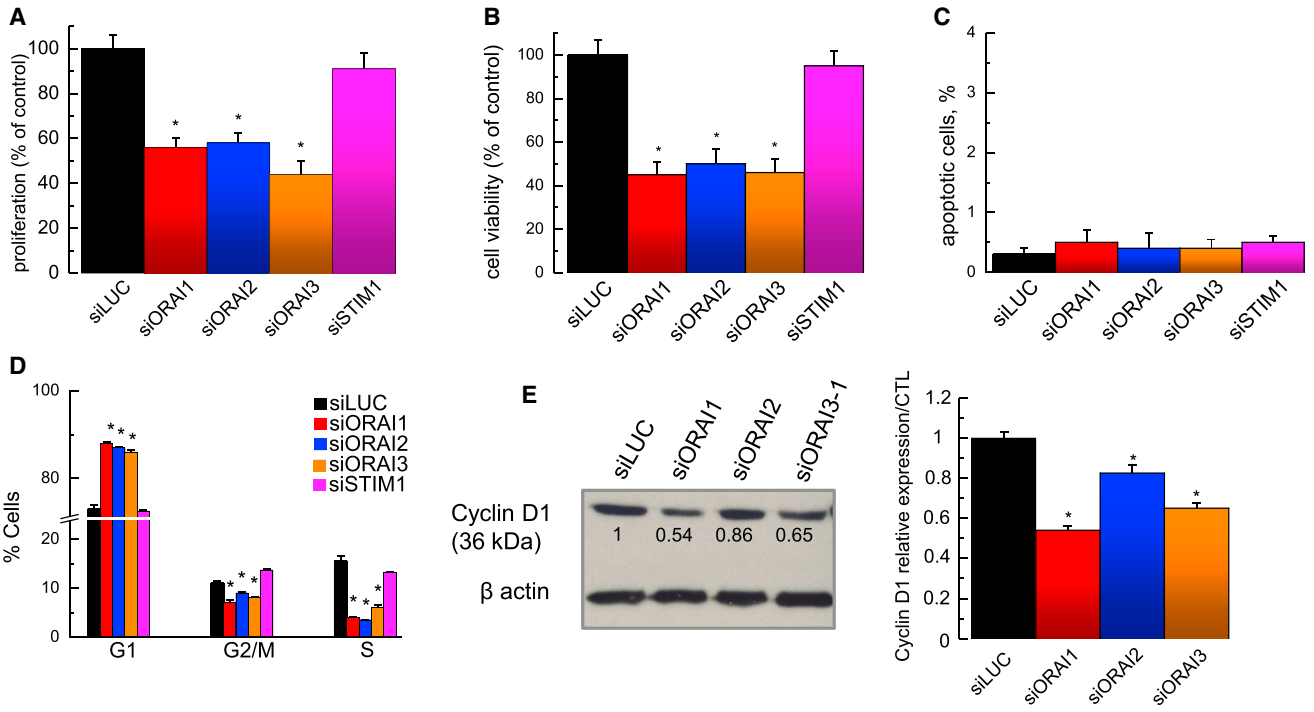

Figure 2. ORAI Isoforms, but Not STIM1, Influence PCa Cell Proliferation and G1 Phase Progression by Downregulating Cyclin D1

(A) The percentage of LNCaP cells proliferating after control, ORAI1-3, or STIM1 knockdown was determined by a colorimetric method (see Experimental Procedures).

(B) Quantification of LNCaP cell viability, as determined by trypan blue exclusion.

(C) Quantification of apoptotic cells, as determined by Hoechst staining, 48 hr after treatment with control or the indicated siRNA.

(D) The cell-cycle distribution of LNCaP cells treated, as above, with the indicated siRNAs for 96 hr, as determined by flow cytometry.

(E) A representative western blot for cyclin D1 (left) and quantification of cyclin D1 protein levels (right) in siORAI knockdown LNCaP cells. The values represent the relative density of bands compared to the control condition (CTL), which will obviously have a relative density of 1 (n = 3).

*$p < 0.05$. Error bars represent means ± SEM. See also Figure S2.

amount of ER intraluminal Ca^{2+} ($[Ca^{2+}]_{ER}$) available for release is also reduced by ORAI depletion. Similar results were obtained with PC-3 cells (Figures S3A–S3D).

It is well known that decreased $[Ca^{2+}]_{ER}$ triggers ER stress and sets off an unfolded protein response (UPR) associated with the activation of specific ER-resident proteins, such as PERK, ATF-6, and IRE1α (Hetz, 2012). It has been demonstrated that activation of the PERK signaling pathway leads to the inhibition of cyclin D1 expression (Brewer and Diehl, 2000). Western blot analysis has shown that downregulation of ORAI isoforms in LNCaP, DU-145, and PC-3 cells leads to the activation of PERK via phosphorylation in all cell types (Figure 3E; Figure S3E). We can notice that in LNCaP cells there is some variability with the weakest response for siORAI1 (Figure 3E). However, these data are consistent with the notion that ORAI protein deficiency and the associated decrease in $[Ca^{2+}]_{ER}$ induce UPR.

Endogenous Association of ORAI1 and ORAI3 Channels to Form Store-Independent Channels Specifically Gated by Arachidonic Acid in PCa Cells

Because ORAI1, ORAI2, and ORAI3 have been also implicated in the formation of other SOC Ca^{2+} entry channel phenotypes (Smyth and Putney, 2012; Várnai et al., 2009; Hogan et al., 2010; Cahalan, 2009), we next asked what kind of molecular interactions among ORAI proteins may underlie the observed changed in Ca^{2+} homeostasis and proliferation of PCa cells. Whether ORAI2 alone, in combination with ORAI1 or with yet unidentified protein(s), forms a distinct store-operated channel in certain cell types is still a matter of debate. In our hands, ORAI2 appeared not to be involved in the endogenous SOCE in PCa cells. However, our data clearly showed that ORAI2 knockdown reduces resting levels of $[Ca^{2+}]_c$ (Figure 3A; Figure S3A), as is consistent with its function in supporting some sort of background steady-state Ca^{2+} influx into PCa cells. As far as ORAI1 and ORAI3 are concerned then, they can also assemble into a 3×ORAI1 plus 2×ORAI3 heteropentamer that underlies the unique type of calcium channel, namely the arachidonic acid-activated channel (ARC) (Mignen et al., 2009).

Figure 4A shows that the application of exogenous arachidonic acid (AA) (8 μM) to LNCaP cells with an approximately 60 s delay activated an inward current that reached a maximal amplitude of 0.93 ± 0.07 pA/pF (n = 7, at membrane potential V_m = −100 mV, Figure 4B) within approximately another 60 s. This current demonstrated the current-voltage (I-V) relationship with marked inward rectification and a very positive reversal potential (Figures 4C and 4D). siRNA-mediated silencing of either ORAI1 or ORAI3 significantly suppressed I_{AA} in LNCaP cells

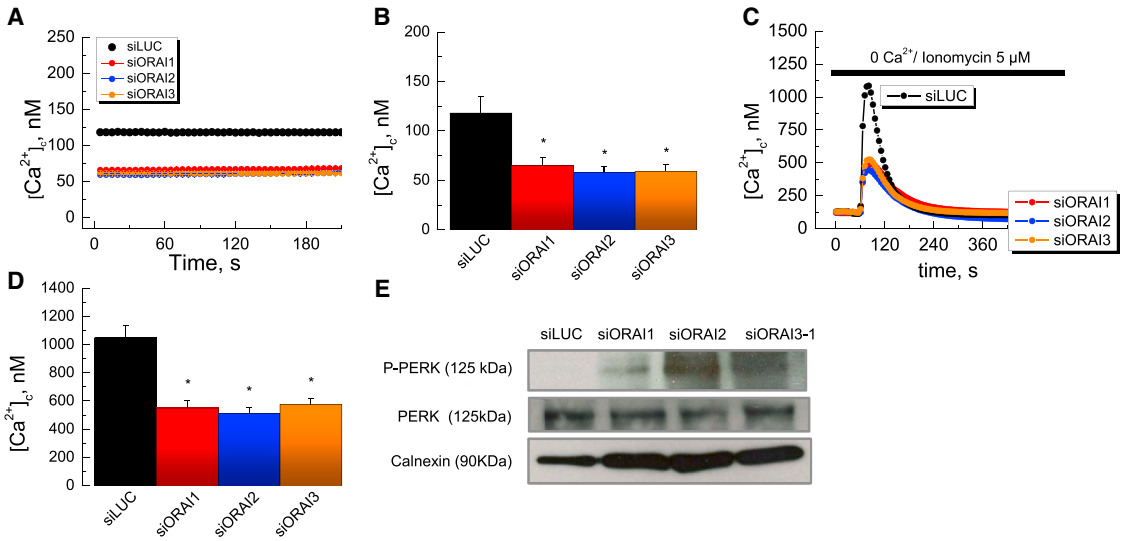

Figure 3. ORAI Isoform Knockdown Induces a Decrease in Both Cytosolic and Reticular Calcium Concentration Combined with ER Stress

(A) Resting $[Ca^{2+}]_c$ signals in LNCaP cells subjected to siRNA-mediated silencing (48 hr) of the indicated ORAI isoforms compared to control (siLUC).

(B) Quantification of resting $[Ca^{2+}]_c$ (n > 150 for each condition).

(C) Representative recordings of IM-induced $[Ca^{2+}]_c$ elevation in LNCaP cells.

(D) Quantification of ER Ca^{2+} content (n > 100 for each condition) from the experiments presented in (C).

(E) Representative western blot of phospho-PERK (P-PERK) in LNCaP cells transfected with control (siLUC) siRNA or siRNA against ORAI isoforms (48 hr; n = 3).

*,p < 0.05. Error bars represent means ± SEM. See also Figure S3.

(Figures 4A and 4B), indicating the requirement of both ORAI isoforms to support this current.

Activation of Ca^{2+} entry by AA in LNCaP cells was further confirmed in calcium imaging experiments in LNCaP cells. As shown in Figure 4E, exposure of LNCaP cells to AA (8 μM) induced a slow rise in $[Ca^{2+}]_c$ up to more than 300 nM. The addition of AA together with La^{3+} (100 μM), which is a potent inhibitor of a number of Ca^{2+}-selective PM channels (Shuttleworth and Thompson, 1998; Mignen and Shuttleworth, 2000), largely prevented AA-induced $[Ca^{2+}]_c$ rise (Figure S4A). Moreover, siRNA-mediated silencing of either ORAI1 or ORAI3, but not ORAI2 in PC-3 cells, significantly reduced the calcium influx elicited by AA (Figure 4F).

AA can be generated endogenously in response to a stimulation of M3 muscarinic receptors (M3-AChR) (Shuttleworth and Thompson, 1998). Application of the nonselective muscarinic agonist, oxotremorine (Oxo, 10 μM), largely mimicked the $[Ca^{2+}]_c$ rise in PC-3 cells induced by exogenous AA (Figure S4B). Moreover, Oxo-induced Ca^{2+} influx in PC-3 cells could be eliminated by siORAI1 or siORAI3 treatment (Figure S4B). Previous studies on ARC channels have shown that they are dependent on STIM1 levels (Mignen et al., 2008), but our results show that siRNA knockdown of STIM1 did not alter AA-activated Ca^{2+} entry (Figure S4C). Therefore we performed biotinylation assays against STIM1 under basal conditions and following TG or AA treatment in PC-3 and HEK-293 cells (Figure S4D). There was no expression of STIM1 at the plasma membrane as was suggested for the activation of classical ARC channels. Finally, we performed additional coimmunoprecipitation assays showing that in contrast to ORAI1, ORAI3 does not coimmunoprecipitate with STIM1 under TG exposure in PC-3 cells (Figure S4E). Collectively, these data confirmed that in prostate models, the mechanism of AA-controlled calcium entry is different from the classical ARC channel described by Mignen et al. (2008, 2009). For these reasons, in the present study, we maintained the term "heteromeric association of ORAI1/ORAI3" instead of ARC.

We next examined whether AA per se can stimulate PCa cell growth. As shown in Figure 4G and in Figure S4F, AA or Oxo were indeed able to stimulate growth of control PC-3 cells (i.e., transfected with anti-luciferase siRNA [siLUC]), whereas the proliferation of PC-3 cells transfected with either siORAI1, siORAI3-1, or siORAI3-2, despite the presence of AA or Oxo, was greatly reduced.

ORAI3 Controls PCa Cell Proliferation via Ca^{2+}/NFAT-Dependent Pathways

We have previously shown that promotion of human primary PCa epithelial cell proliferation via TRPC6 or TRPV6 channel-mediated Ca^{2+} entry, involves the activation of a Ca^{2+}-dependent transcription factor, which is the nuclear factor of activated T-cells (NFAT) (Thébault et al., 2006; Lehen'kyi et al., 2007). In our case, incubation of PC-3 cells with the cell-permeable NFAT inhibitor peptide (VIVIT; 50 μM for 3 hr) was able to abolish AA-stimulated proliferation (Figure 4G). Next, we proceeded to measuring NFAT transcriptional activity in response to the alterations in AA-induced Ca^{2+} entry caused by impairment of ORAI3 expression. In these experiments, LNCaP or PC-3 cells were cotransfected with siORAI3 and pCIS-CK plasmid containing an insert of a luciferase reporter gene driven by a synthetic NFAT-dependent promoter (pNFAT-Luc plasmid). Figure 4H, S4G, and S4H show that incubation of pNFAT-Luc-transfected LNCaP or PC-3 cells in media containing AA (3 μM) or Oxo (10 μM) results in greater luciferase light emission than in cells not exposed to AA or Oxo. AA- or Oxo-stimulated luciferase activity could be greatly reduced by siRNA-mediated ORAI3

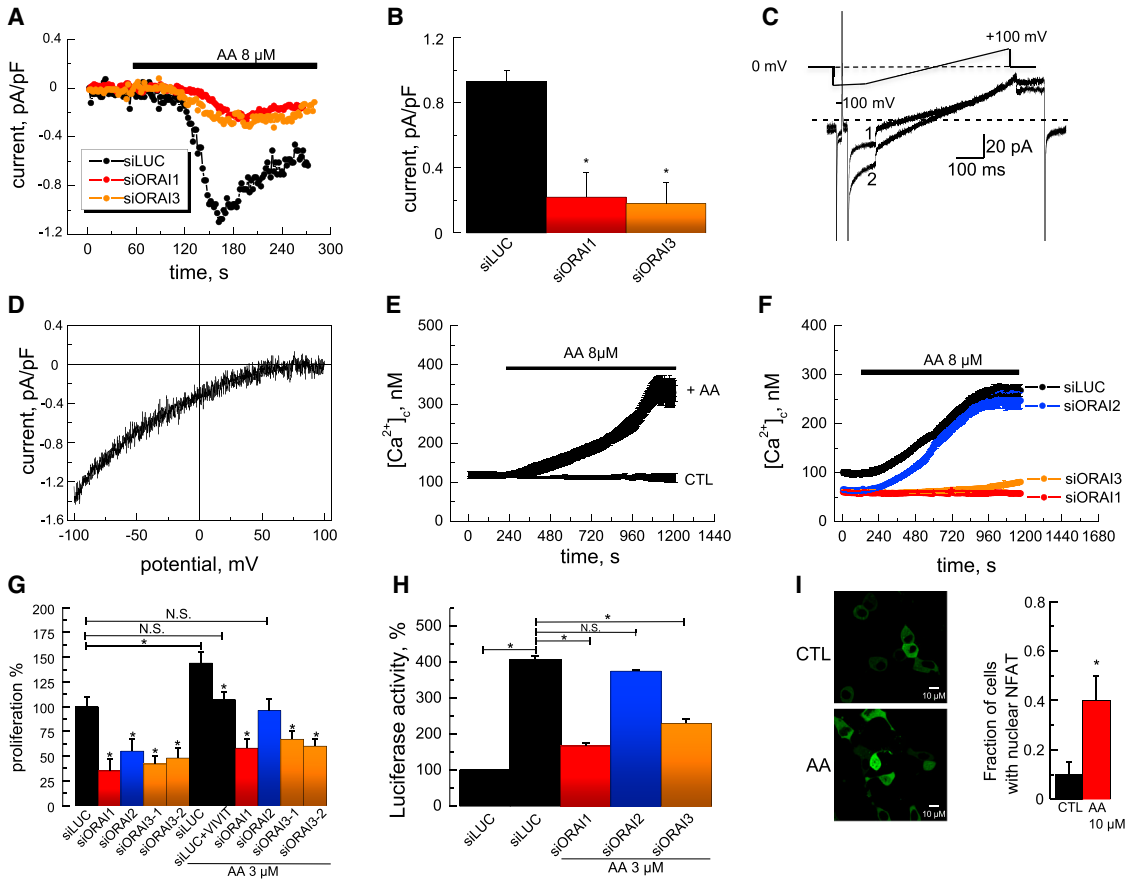

Figure 4. Endogenous Association of ORAI1 and ORAI3 Leads to the Formation of Store-Independent, AA-Regulated Channels Involved in Stimulation of Proliferation via NFAT Signaling.

(A) Representative time courses of the development of inward current in response to AA application in LNCaP cells subjected to the indicated siRNA-mediated silencing (48 hr). Current amplitude was measured at −100 mV at the onset of hyperpolarization (see C).

(B) Quantification of current amplitudes shown in (A; n > 6 for each condition).

(C) Representative original traces of base-line current (1) and fully developed current in LNCaP cells in response to AA (8 μM) application (2) in LNCaP cell together with the voltage protocol used to elicit the currents.

(D) I-V relationship of a fully-developed current derived from the traces presented in (C).

(E) $[Ca^{2+}]_c$ rise in LNCaP cells in response to AA (horizontal bar). CTL, control.

(F) $[Ca^{2+}]_c$ responses of control PC-3 cells (siLUC) and PC-3 cells subjected to anti-ORAI isoform-specific siRNAs treatment (48 hr) to AA.

(G) Quantification of the percentage of baseline and AA-stimulated proliferation of control PC-3 cells. Pretreatment with the cell-permeable NFAT inhibitor peptide (VIVIT; 50 μM; 3 hr) abolished AA-mediated proliferation.

(H) Quantification of luciferase-reported baseline and AA-stimulated NFAT activity in PC-3 cells.

(I) Confocal images of NFAT-GFP fluorescence in live PC-3 cells transiently transfected with NFAT-GFP during vehicle control (CTL, upper panel) or AA (lower panel) application showing AA-induced NFAT translocation to the nucleus.

*$p < 0.05$. Error bars represent means ± SEM. See also Figure S4.

silencing. In addition, AA caused translocation of NFAT to the nucleus, as was assayed on PC-3 cells transiently transfected with NFAT-GFP construct (Figure 4I). Overall, the results of these experiments strongly suggested that endogenous AA-activated channels in PCa cells formed by ORAI1 and ORAI3 proteins are highly likely to be involved in cell proliferation, by providing the Ca^{2+} entry required for the induction of transcriptional activity of the Ca^{2+}-dependent transcription factor, NFAT.

ORAI1/ORAI3 Ratio Modulates Basal $[Ca^{2+}]_c$ and Size of SOCE

To further characterize the significance of ORAI3 in the maintenance of Ca^{2+} homeostasis, we took advantage of the fact that PC-3 cells express lower levels of endogenous ORAI3 mRNA (Figure S5A) than LNCaP cells do (see Figure S1D). As shown in Figure 5A, transient overexpression of ORAI3 in PC-3 cells resulted in the notably higher resting $[Ca^{2+}]_c$ levels than in the control PC-3 cells at regular 2 mM external Ca^{2+} concentrations ($[Ca^{2+}]_o$; see also Figure S5B). Moreover, increasing $[Ca^{2+}]_o$ in the bathing solution from 0 to 10 mM produced more significant elevations of the basal $[Ca^{2+}]_c$ in ORAI3-overexpressing PC-3 cells than in the control ones (Figure 5A; Figure S5C). This would suggest that ORAI3 specifically promotes enhanced basal Ca^{2+} influx and not Ca^{2+} liberation from intracellular sources. Intriguingly, the use of TG (1 μM) for the selective activation of SOCE showed that ORAI3 overexpression resulted not in the increase

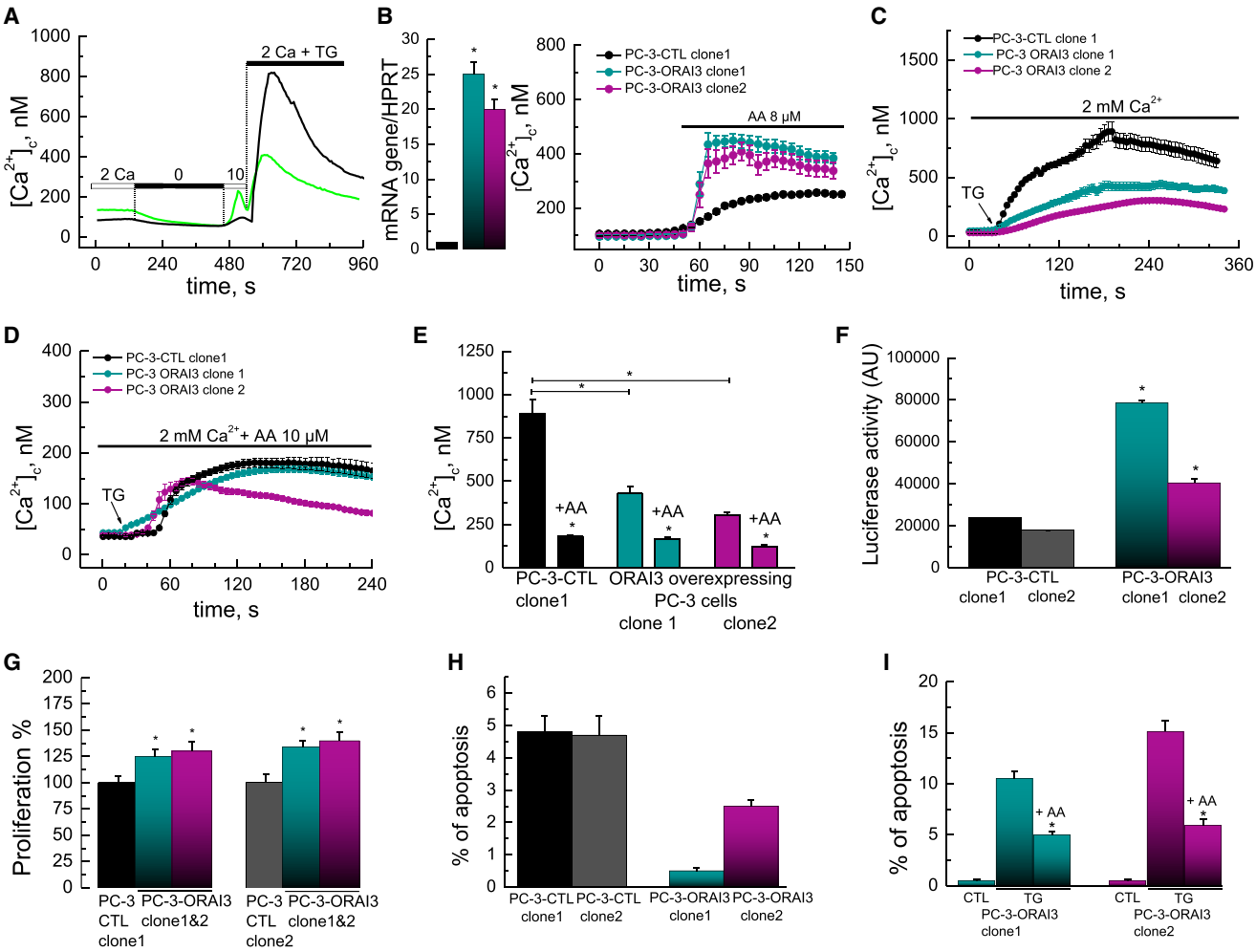

Figure 5. Both the ORAI1/ORAI3 Ratio and AA-Regulated Ca^{2+} Entry Promote Apoptosis Resistance and Cell Proliferation by Controlling basal $[Ca^{2+}]_c$ and Amplitude of SOCE

(A) $[Ca^{2+}]_c$ in the presence of 0, 2, or 10 mM extracellular Ca^{2+} and after TG treatment in PC-3 cells transiently overexpressing ORAI3 (green line) compared to control cells (black line).

(B) Quantification of ORAI3 mRNA in two PC-3 clones stably overexpressing ORAI3 relative to a control clone (PC-3-siLUC clone 1). Both clones showed higher AA-stimulated calcium entry (right panel).

(C and D) $[Ca^{2+}]_c$ responses of PC-3-CTL clone 1 and PC-3-ORAI3 clone 1 and clone 2 cells to TG (1 μM) alone (C) or after pretreatment with AA (D, 25 min of treatment with 10 μM AA).

(E) Quantification of $[Ca^{2+}]_c$ responses from experiments presented in (C and D) ($n > 100$ for each condition).

(F) Quantification of the effects of ORAI3 overexpression in PC-3 cells on luciferase-reported baseline NFAT activation.

(G) Quantification of the percentage of baseline proliferation of control and ORAI3-overexpressing PC-3 clones ($n = 3$) for each clone.

(H and I) Quantification of TG-induced apoptosis [0.5 μM/48 hr (H); 2 μM/48 hr (I)] of control and ORAI3-overexpressing clones and with AA treatment (3 μM; $n = 3$) for each clone.

*$p < 0.05$. Error bars represent means ± SEM. See also Figure S5.

but also in the decrease of the $[Ca^{2+}]_c$ signal associated with SOCE in PC-3 cells (Figure 5A; Figure S5D). Because both ORAI1 and ORAI3 can potentially be involved in SOCE, these results indicate that ORAI3 overexpression, on the one hand, leads to the enhancement of the basal store-independent Ca^{2+} entry and, on the other hand, suppresses the store-dependent one. Such a situation can only be explained if we conclude that higher ORAI3 levels, in the presence of a limited ORAI1 supply, favor the formation of heteromeric ORAI1-ORAI3-based channels, thence contributing to the basal, nonstimulated influx of Ca^{2+} at the expense of homomeric ORAI1- or ORAI3-based SOCs.

In LNCaP cells, neither overexpression of ORAI3 nor its siRNA-mediated knockdown had any significant impact on the size of TG-activated SOCE (Figure S5E). The lack of the influence of ORAI3 overexpression on SOCE amplitude in LNCaP cells was most probably explained by the higher basal expression of ORAI3 than in PC-3 cells. When control LNCaP cells were exposed to AA (10 μM), the cytosolic calcium concentration slowly increased (Figure S5F). The subsequent addition of TG

(1 μM) revealed much less SOCE than in LNCaP cells not stimulated with AA (Figure S5E). We also confirmed these data on primary human prostate cancer cells (Figure S5G–S5I). Finally, we performed coimmunoprecipitation assays showing that ORAI3 overexpression (PC-3-ORAI3 clone 1) virtually abolished ORAI1 coimmunoprecipitation with STIM1 under TG exposure compared with PC-3-CTL clone 1 (Figure S5J). Collectively, these data strongly suggest that the activation of endogenous store-independent channels by AA recruits ORAI1 isoforms to oligomerize with ORAI3, thereby inhibiting SOCE.

ORAI3 Overexpression Stimulates Cell Proliferation and Promotes Apoptosis Resistance

To further investigate the significance of ORAI3 in Ca^{2+} signaling and cancer cell growth, we produced PC-3 cells with stable ORAI3 overexpression. To avoid clonal variations in the properties, two clones of PC-3 cells that overexpress ORAI3, PC-3-ORAI3 clone 1 and PC-3-ORAI3 clone 2, and two clones, PC-3-CTL clone 1 and PC-3-CTL clone 2, which served as respective controls, were created and analyzed. Overexpression of ORAI3 mRNA in PC-3-ORAI3 clone 1 and clone 2 cells was confirmed by real-time PCR (Figure 5B, left panel). As with transient ORAI3 overexpression in PC-3 cells, both clones showed higher AA-stimulated calcium entry (Figure 5B, right panel) and lower TG-stimulated SOCE (Figure 5C) than in the respective controls. This was most likely due to the preferred formation of endogenous store-independent Ca^{2+} channel specifically gated by AA at the expense of homomeric ORAI1- or ORAI3-based SOCs. Moreover, a greater reduction of TG-activated SOCE in either control or ORAI3-overexpressing clones of PC-3 cells could be achieved by cell pretreatment with AA (25 min with 10 μM AA) (Figures 5D and 5E). This is consistent with the notion that AA per se serves as a promoting factor for ORAI1 and ORAI3 heteromerization. In addition to this, luciferase assay revealed much higher basal NFAT activity in PC-3-ORAI3 clone 1 and clone 2 cells (Figure 5F), as well as their significantly enhanced AA-stimulated proliferation when compared to the respective controls (Figure 5G).

Our previous studies have shown that enhanced apoptosis resistance of androgen-independent PCa cells is largely conferred by their reduced SOCE (Vanden Abeele et al., 2002; Prevarskaya et al., 2004; Flourakis et al., 2010). In full agreement with this fundamental finding, both PC-3-ORAI3 clone 1 and PC-3-ORAI3 clone 2, which had their SOCE reduced, demonstrated lower sensitivity to the TG-induced apoptosis (Figure 5H). Increasing concentrations of TG to 2 μM significantly enhanced apoptosis of PC-3-ORAI3 clone 1 and clone 2 cells (Figure 5I). However, cotreatment with AA exerted a greater protective effect (Figure 5I), most likely because of promotion by AA of ORAI1 isoforms to oligomerize with ORAI3, thereby resulting in a greater reduction in SOCE (Figures 5D and 5E).

The Dynamics of ORAI1 and ORAI3 Subcellular Distribution in PCa Cells

To locate ORAI1 and ORAI3 proteins, we performed confocal imaging of PC-3 cells immunostained with anti-ORAI1 (green) and anti-ORAI3 (red) antibodies. After treatment with TG (1 μM, 5 min) ORAI1 staining became notably denser at the cell's periphery (Figure 6A). The addition of AA (10 μM) to the incubation medium had no visible effect on the pattern of ORAI1 and ORAI3 staining. The addition of AA (10 μM) together with TG (1 μM) to the incubation medium partially reversed the peripheral ORAI1 staining induced by TG with little effect on the pattern of ORAI3 staining. In ORAI3-overexpressing PC-3 cells (Figure 6B), transition to heavy peripheral ORAI1 staining in response to TG (1 μM) was prevented. AA, when applied alone, induced a formation of hemisphere-shaped areas of ORAI1 and ORAI3 staining. Finally, in ORAI3-overexpressing PC-3 cells, AA (10 μM) was also able to completely prevent any heavy peripheral ORAI1 staining induced by TG (1 μM). Original traces (Figure S6A) and histograms (Figures S6B–S6D) show quantification of the peripheral peak of ORAI1 and ORAI3 fluorescence. These data suggest an impairment of the SOCE mechanism induced by AA.

Treatment of PCa Cells with Arachidonic Acid Enhanced the Association between ORAI1 and ORAI3.

We also investigated membrane targeting and association of ORAI1 and ORAI3 in PC3 cells. Cell-surface biotinylation of PC3 cells treated with AA or Oxo showed no significant variation in plasma membrane ORAI3 expression, ruling out its possible rapid translocation to plasma membrane (Figure 6C). AA or Oxo treatments of PC-3 cells also did not change ORAI3 protein expression (Figure 6D). In addition, coimmunoprecipitation from lysates of PC3 cells with either anti-ORAI1 (Figure 6E, left panel) or anti-ORAI3 (Figure 6E, right panel) antibodies showed formation of endogenous heteromeric complexes by ORAI1 and ORAI3 proteins. Moreover, Ca^{2+} store depletion by TG decreased the association of ORAI1 with ORAI3 (Figure 6F, middle panel), whereas a consecutive treatment with AA (10 μM, 30 min) and TG (1 μM, 10 min) promoted such association (Figure 6F, right panel). In a complementary series of experiments, we sought to strengthen our hypothesis that ORAI3 overexpression alone without any AA treatment is sufficient to promote basal ORAI1 oligomerization with ORAI3, resulting in an inhibition of SOCE. In this series, we transiently overexpressed different ratios of ORAI1, STIM1, and ORAI3 in prostate cancer cells to mimic what happens during prostate cancerogenesis and examined how it affects ORAI1 and STIM1 coimmunoprecipitation, as well as SOCE under TG exposure (Figures S6E and S6F). They show that at a ratio of 1:1:1 (1 μg of each plasmid per 2 ml petri dish), SOCE becomes decreased by approximately 38% compared to a ratio 1:1:0, indicating that just the presence of ORAI3 is sufficient to inhibit SOC-mediated calcium entry. Increasing the proportion of ORAI3 by a factor of 3 (i.e., to a ratio 1:1:3), typical of prostate carcinogenesis, produced even stronger inhibition of SOCE amplitude by approximately 62%.

We next used ORAI1-YFP construct to enable ORAI1 tracing in PC-3 cells in confocal imaging experiments during overexpression of different ratios of ORAI1, ORAI3, and STIM1 (see Figures S6G and S6H). At a 1:1:0 ratio, ORAI1 staining showed quite diffused distribution under control condition, but after treatment with TG (1 μM, 5 min), the staining became notably denser at the cell's periphery. At a ratio of 1:1:1, peripheral ORAI1 staining induced by TG was partially reversed, whereas at a ratio of 1:1:3, TG virtually failed to induce peripheral ORAI1 staining.

Finally, we performed coimmunoprecipitation assays showing that at a ratio 1:1:3 ORAI3 overexpression decreases ORAI1 coimmunoprecipitation with STIM1 under TG exposure compared

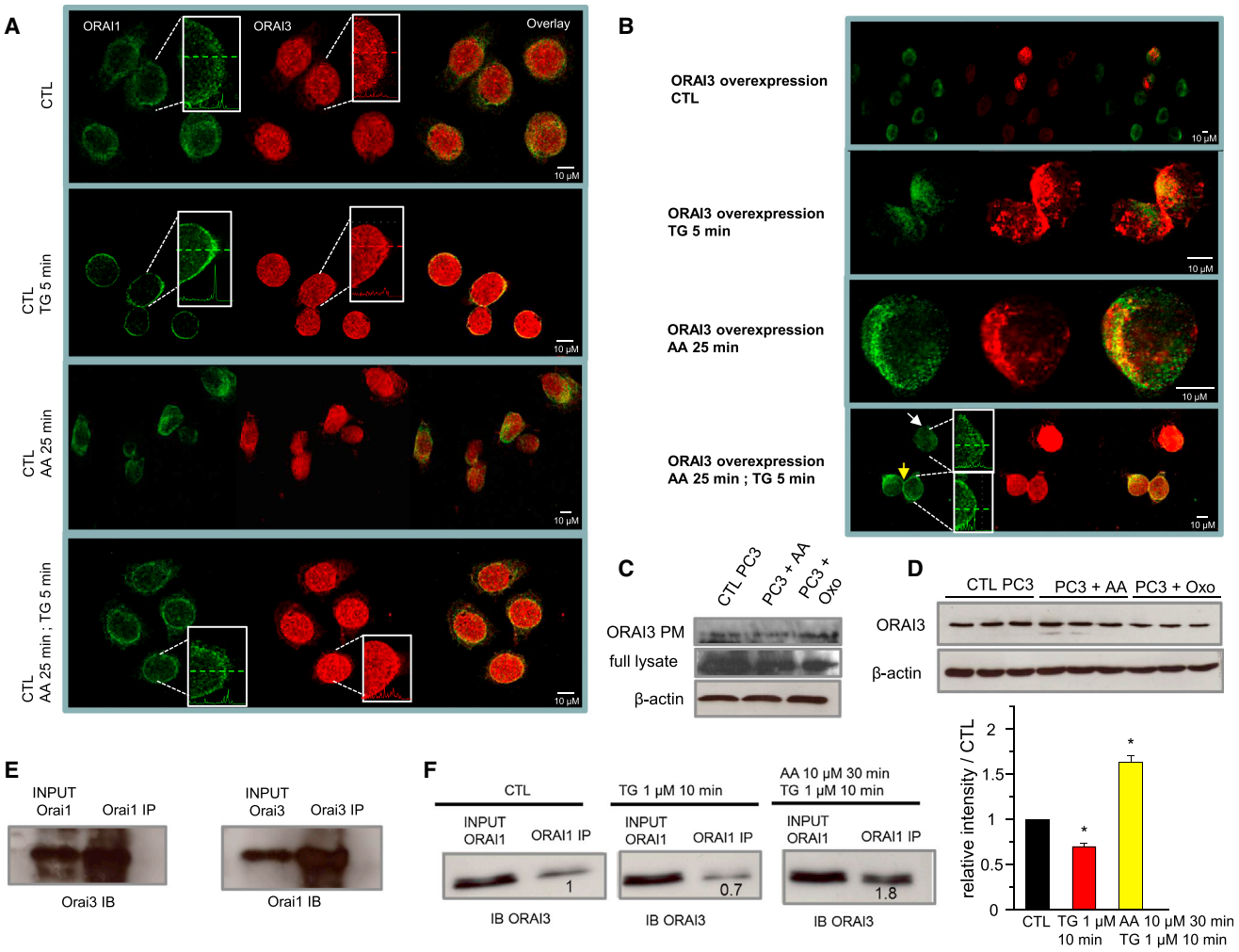

Figure 6. ORAI1/ORAI3 Ratio and AA-Regulated Ca^{2+} Entry Control the Dynamics of ORAI1 and ORAI3 Subcellular Distribution

(A) Confocal images of immunocytochemical detection of ORAI1 (green), ORAI3 (red), and merged images (yellow) in resting state wild-type PC3 cells and at the indicated time after treatment with 1 μM TG, with 10 μM AA, or with consecutive AA (10 μM) and TG (1 μM) treatment.

(B) Images as in (A), but for PC-3 cells with transient ORAI3 overexpression. The yellow arrow indicates untransfected cells, and white rectangles present the fluorescence intensity of ORAI1 or ORAI3 from the shown selected and magnified areas.

(C) Western blots of ORAI3 in total (full lysate) and biotinylated (PM) protein fractions of control (CTL) treated PC3 cells and following treatment with AA (8 μM) or Oxo (10 μM) for 30 min (n = 3).

(D) Western blots of ORAI3 protein levels in CTL treated PC-3 cells and cells pretreated with AA or Oxo (n = 3).

(E) Immunoblots (IB) for ORAI3 (left) or ORAI1 from total PC3 cell lysates (input) or lysates immunoprecipitated (IP) with either ORAI1 or ORAI3 antibodies (n = 3).

(F) IB for ORAI3 from lysates immunoprecipitated with ORAI1 and following indicated treatments. The values represent the relative density of bands compared to the ORAI1 IP fraction in control condition, which will obviously have a relative density of 1 (n = 3).

*$p < 0.05$. Error bars represent means ± SEM. See also Figure S6.

to a ratio of 1:1:1. (Figure S6I). Collectively, these data strongly support our hypothesis that either ORAI3 overexpression or AA per se serve to promote ORAI1 oligomerization with ORAI3, resulting in the formation of endogenous store-independent Ca^{2+} channel specifically gated by AA with a simultaneous inhibition of SOCE.

Oncogenic Role of ORAI3 in Xenograft Tumor Assays

Our results suggest that ORAI3 protein can be regarded as an oncogenic one, because its overexpression, on the one hand, favors the formation of a PM Ca^{2+}-permeable channel that stimulates PCa cell proliferation and, on the other hand, disfavors the expression of the channel that is important in supporting susceptibility to apoptosis. We conducted experiments on mouse prostate tumor xenografts using the strategy of siRNA-mediated ORAI3 knockdown. In our experiments, to achieve ORAI3 knockdown, mice with PC-3 cell-induced xenograft tumors were injected intraperitoneally (i.p.) on a daily basis with two different anti-ORAI3 siRNAs: siORAI3-1 and siORAI3-2 (to exclude nonspecific effects of siRNAs). Results of these experiments have shown that siRNA-treated animals displayed significantly reduced tumor growth compared with the animals treated with

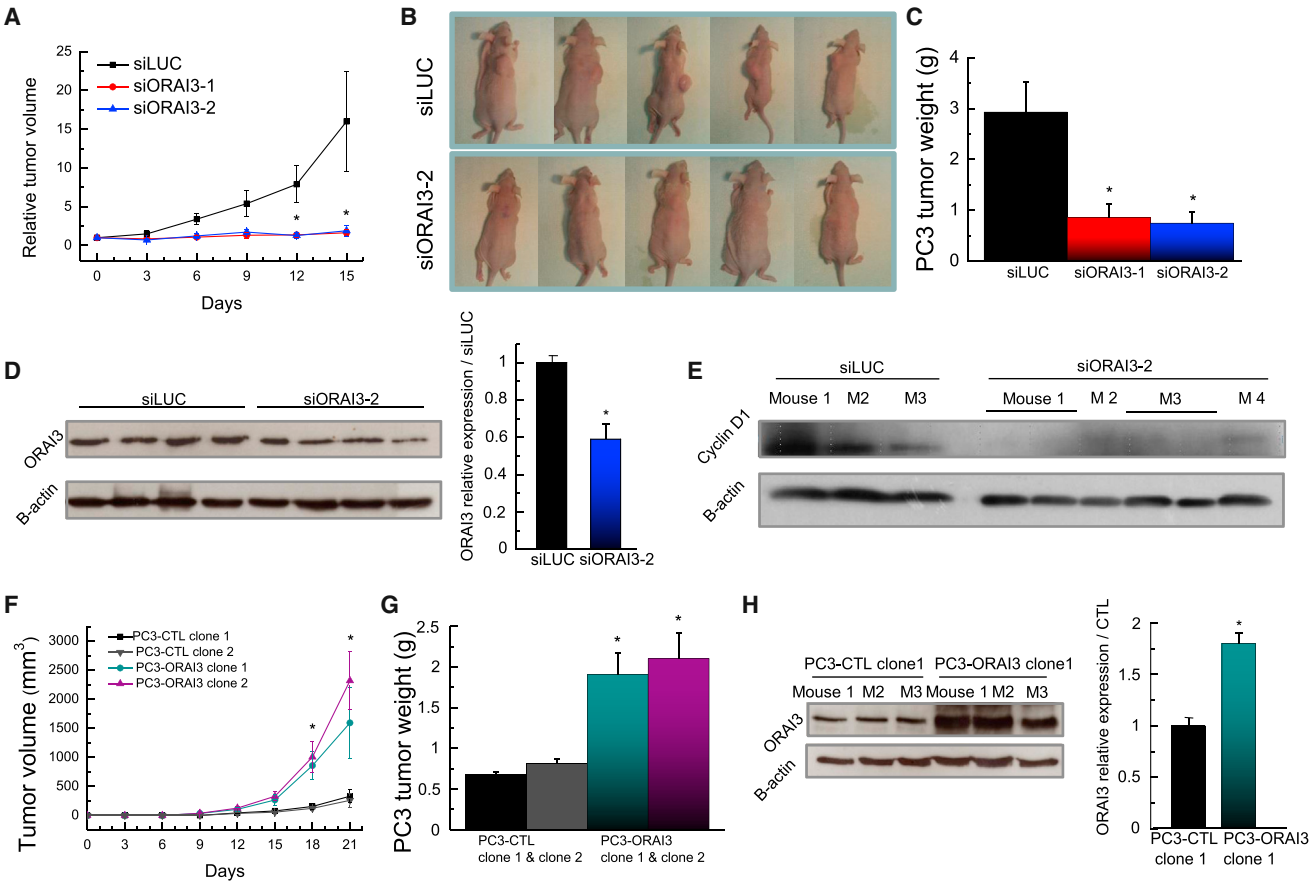

Figure 7. The Effects of ORAI3 on In Vivo Xenograft Tumors

(A) The relative volume of PC-3 cell xenograft tumors over time in nude mice treated for 2 weeks with control siLUC (n = 7) or with two siRNAs against ORAI3 (siORAI3-1, n = 6; and siORAI3-2, n = 6).

(B) Representative photographs of the indicated siRNA-treated and untreated animals.

(C) Xenograft tumor weights after 2 weeks of siRNA treatment.

(D and E) Western blots showing ORAI3 (D, left panel) and cyclin D1 (E) protein levels in siLUC and siORAI3-2 PC3 tumors. ORAI3 relative expression normalized to levels of β-actin is shown (D, right panel).

(F and G) Tumor volume over time (F) and tumor weight (G) from two control (PC-3-CTL clone 1 and 2) and two ORAI3-overexpressing clones (PC-3-ORAI3 clone 1 and PC-3-ORAI3 clone 2) 3 weeks after xenograft induction in nude mice (n = 6 for each tumor type).

(H) ORAI3 protein expression in PC-3-CTL clone 1 and PC-3-ORAI3 clone 1 tumors as determined by western blot.

*$p < 0.05$. Error bars represent means ± SEM. See also Figure S7.

siLUC (Figures 7A–7C). The inhibition of tumor growth in mice treated with anti-ORAI3 siRNAs correlated with a downregulation of ORAI3 protein (Figure 7D) and cyclin D1 expression (Figure 7E), which would suggest that specific therapeutic targeting of ORAI3 affects cancer cell proliferation. In contrast, mouse xenografts from either PC-3-ORAI3 clone 1 or clone 2 cells were characterized by accelerated tumor growth (Figure 7F), higher tumor weight (Figure 7G), and overexpression of ORAI3 (Figure 7H). We also conducted additional series of in vivo experiments, in which the effects of ORAI1 silencing in PC-3-ORAI3 clone 1 cells was examined. These experiments have demonstrated an inhibition of tumor growth in mice treated with siORAI1 (Figure S7A), which correlated with a downregulation of cyclin D1 (Figures S7B and S7C) and ORAI1 expression (Figures S7B and S7D). Thus, the enhanced tumor growth observed with ORAI3 overexpression (Figure 7F) appears to be not only ORAI3-dependent, but also dependent on the pool of ORAI1 protein, which, at least in part, can be explained by the requirement of heteromeric ORAI1/3 channel formation for sustaining such growth.

DISCUSSION

In this study, we report four findings for the understanding of the Ca^{2+} dependence of prostate carcinogenesis (Figure 8). ORAI1 is the key subunit involved in the formation of homomultimeric plasma membrane SOC in PCa epithelial cells. PCa progression is associated with enhanced ORAI3 protein expression. An increased level of endogenous ORAI3 protein in PCa cells favors the preferred association of ORAI3 with ORAI1 to form heteromultimeric store-independent AA-regulated channels at the expense of homomultimeric ORAI1-based SOCs. Also, derivation of AA-regulated channels at the expense of SOCs caused by altered ORAI1/ORAI3 ratio represents an oncogenic switch in preferred Ca^{2+} entry pathway that promotes PCa cell

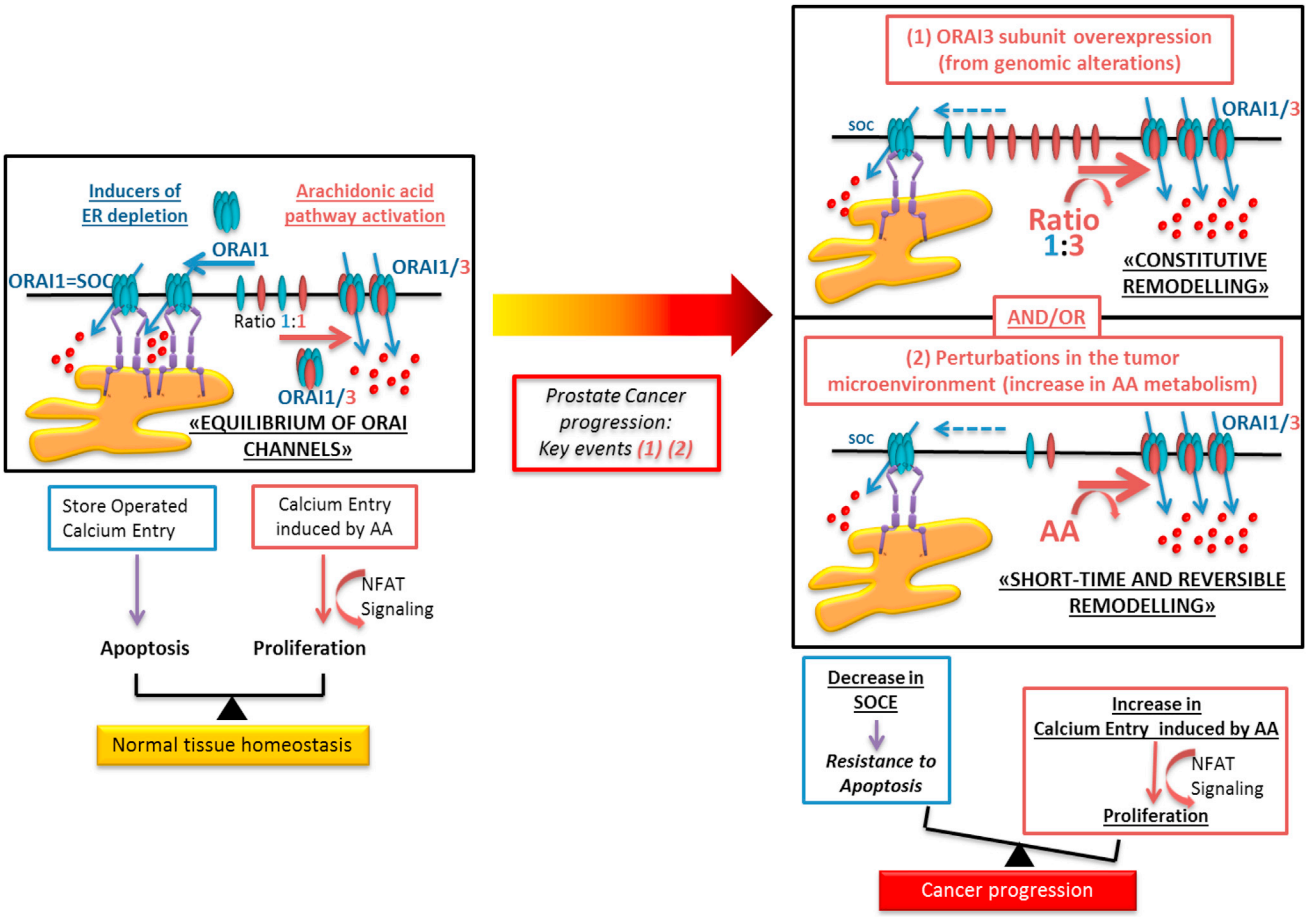

Figure 8. Disrupted Dynamic Equilibrium of ORAI Channels Simultaneously Contributes to Two Cancer Hallmarks: Enhanced Growth and Resistance to Apoptosis

proliferation and confers apoptosis resistance. These findings demonstrate the functional significance of store-independent AA-regulated channels in cancer cells in providing the Ca^{2+} influx required for cells proliferation and the switch to an oncogenic phenotype.

Arachidonic Acid-Regulated Channels in Prostate Cancer Cells

The concept of ARC emerged in 2000 (Mignen and Shuttleworth, 2000), based on the previous series of studies of agonist-evoked Ca^{2+} entry in response to the low agonist concentrations, insufficient to produce substantial emptying of the ER Ca^{2+} stores. It was established that the messenger responsible for the activation of Ca^{2+} entry under these circumstances is a receptor-stimulated derivation of AA. With the discovery of STIM and ORAI proteins as critical determinants of Ca^{2+} entry mechanisms in nonexcitable cells, it was also determined that the "classical" functional ARC channel is formed by a heteropentameric assembly of three ORAI1 and two ORAI3 subunits, whose activation also requires the constitutive presence of a discrete pool of PM-resident STIM1 (Mignen et al., 2009). Our data suggest that overexpression of ORAI3 in PCa cells leads to the derivation of Ca^{2+}-permeable channels with similar subunit composition and functional features to classical ARC channels, yet we may already say that such overexpression shifts the balance in preferred Ca^{2+} entry pathways from store-dependent ones to those whose activation is dependent on AA. Indeed, the biophysical properties of the corresponding membrane current in PCa cells, such as strong inward rectification and lack of distinct reversal potential, are similar to those described previously for ARC (Mignen and Shuttleworth, 2000; Mignen et al., 2009). However, our results show that siRNA knockdown of STIM1 does not alter AA Ca^{2+} signaling. Moreover, neither coimmunoprecipitation nor biotinylation assays were able to confirm the implication of STIM1 in the mechanism of AA-mediated calcium entry in PCa cells. These results suggest that in prostate models, the mechanism of AA-mediated calcium entry differs from the classical ARC channel described by Mignen et al. (2009). For these reasons, in the present study, we maintained the term "heteromeric association of ORAI1/ORAI3" instead of ARC.

Functional Significance of AA-Activated Ca^{2+} Influx in Prostate Cancer Cells

We also demonstrated that the signaling pathway via which AA-activated Ca^{2+} influx promotes proliferation of PCa cells involves the activation of a Ca^{2+}/calcineurin-dependent transcription

factor, NFAT, followed by the stimulation of the expression of the key rate-limiting controller of G1/S phase transition, cyclin D1. Thus, in terms of a preferential effect on proliferation, ORAI1/ORAI3-based channels in PCa cells are quite similar to TRPC6 channels, which have also been shown to support the Ca^{2+} entry that is specifically linked to NFAT-mediated transcriptional activity promoting the expression of cell cycle regulators (Thébault et al., 2006). However, the activation of TRPC6 is coupled to α1-adrenoreceptor (α1-AR) signaling (Thébault et al., 2006), whereas here we show that endogenous store-independent ARC activation is associated with muscarinic mAChR-stimulated derivation of AA. This suggests that stimulation of both types of receptors, α1-AR and mAChR, confer greater proliferation on PCa cells, and consequently the suppression of α1-AR- and/or mAChR-mediated signaling may be considered as adjuvant therapy in PCa treatment.

Moreover, the AA signaling pathway that incorporates phospholipase, cyclooxygenase, lipoxygenase, and epoxygenase enzymes has been shown to play a major role in the development and progression of a number of cancers (Nakanishi and Rosenberg, 2006), including PCa. The inhibition of AA production has been shown to decrease prostate-specific antigen expression and PCa growth in preclinical studies (Patel et al., 2008). There is also a positive correlation between carcinogenesis and dietary intake of both the omega-6 fatty acid precursor linoleic acid and its product AA (Phinney, 1996). Our work provides a solution to resolve some roles of tumor microenvironment perturbations and the role of nerves in tumor growth and progression in PCa. Indeed, a recent study by Magnon et al. (2013) demonstrated in *in vivo* mouse models of the nerve fibers from the parasympathetic nervous system, which deliver acetylcholine, the role of nerves in tumor growth and progression in PCa. These findings bring evidence suggesting that ORAI3 may represent a therapeutic target in PCa. Considering that we demonstrate that the ORAI1/3 heteromer promotes proliferation following stimulation of M3 muscarinic receptors (M3-AChR), these results fit with the notion that PCa progression mediated by parasympathetic cholinergic fibers is at least partly due to ORAI1/3 heteromers. Thus, our study provides insight into the role of AA in oncogenesis by establishing a direct link between AA metabolism and PCa cells proliferation via the involvement of AA-regulated Ca^{2+} entry.

Role of ORAI Proteins in Prostate Cancer Hallmarks

Our findings reveal a mechanism via which PCa cells, by changing the expression of a single protein (i.e., ORAI3), can simultaneously promote two key oncogenic hallmarks: enhanced growth and increased resistance to apoptosis. Indeed, overexpression of ORAI3, on the one hand, disrupts normal homomultimerization of ORAI1, leading to the decreased density of SOCs and, on the other hand, favors heteromultimerization of ORAI3 and ORAI1, resulting in the derivation of ARC-like AA-regulated channels. Thus, controlling ORAI3 expression can be viewed as a promising strategy in PCa treatment. This notion is supported by the results obtained from mouse prostate tumors.

ORAI3 was also recently implicated in the promotion of proliferation and apoptosis resistance of HBC cells (Faouzi et al., 2011; Motiani et al., 2013). This was attributed to the fact that ORAI3 represents the main SOCE pathway in MCF-7 and T47D HBC cell lines, but not in the normal MCF-10A cells. However, it remains unclear how the same Ca^{2+} entry channel can be simultaneously engaged in two processes with different Ca^{2+} dependence. Our data indicate that in PCa cells ORAI3 determines the oncogenic switch between two Ca^{2+}-channel phenotypes: AA-regulated and store-operated ones, of which the former is important for proliferation and the latter is important for apoptosis providing a solution to controversies in the literature as to the involvement of the ORAI3 channel in SOCE and the role of ORAI3 in cancer progression. We demonstrate that at least two factors control the formation of ORAI monomers or heteromers, namely the channel expression ratio and AA metabolism. Depending on the structure of the channel formed, ORAI channels can function as: (1) a SOC; (2) a constitutively open channel; or (3) a channel activated by AA metabolism. In contrast to Holzmann et al. (2013), we show the overexpression of ORAI3 in cancer tissues leading to the appearance of Ca^{2+} signaling dependent on the endogenous levels and production of AA. Therefore, we establish an oncogenic role for the ORAI3 channel and a mechanism via which AA metabolism is involved in prostate oncogenesis.

EXPERIMENTAL PROCEDURES

Cell Culture

The human PCa cell lines LNCaP, DU-145, and PC-3 were obtained from the American Type Culture Collection and maintained in culture in RPMI 1640 medium (Gibco-Life Technologies) supplemented with 10% fetal calf serum (Seromed, Poly-Labo), 5 mM L-glutamine (Sigma), and kanamycin 100 μg/ml. LNCaP C4-2 cell line was a generous gift from Dr. F. Cabon. Cells were grown at 37°C in a humidified atmosphere containing 5% CO_2. The medium was replaced every 48 hr.

Cancer Tissue Sampling

Prostate tissue samples (prostate adenocarcinoma) were obtained from 15 patients with a mean age of 62.4 years (ranging from 51 to 70) who underwent radical prostatectomy between January 2004 and June 2008 in the department of Urology at Hospital Centre Lyon-Sud (The detailed procedure is presented in Supplemental Experimental Procedures). Noninterventional biomedical research protocol for tissue sample conservation after prostate surgery has been set up at the Centre Hospitalier Lyon-Sud, and the Ethics Committee in Lyon (CPP Sud-Est 2) specifically approved it for this study. The patients admitted to the urology department in the Centre Hospitalier Lyon-Sud were informed and gave voluntary, signed informed consent prior to any tissue sample conservation and for research use.

Electrophysiology and Solutions

The composition of the extracellular solution for patch-clamp recording was 120 mM NaCl, 5 mM KCl, 10 mM $CaCl_2$, 2 mM $MgCl_2$, 5 mM glucose, and 10 mM HEPES, pH 7.4 (adjusted with tetraethylammonium hydroxide), osmolarity was 310 mOsm/kg adjusted with D-mannitol. The patch pipettes were filled with the basic intracellular pipette solution: 120 mM cesium-methane sulfonate, 10 mM CsCl, 10 mM HEPES, 10 mM 1.2-bis(2-aminophenoxy)ethane N,N,N′,N′-tetraacetic acid (BAPTA), and 6 mM $MgCl_2$ (pH adjusted to 7.4 with CsOH, and osmolarity was 295 mOsm/kg adjusted with D-mannitol). In whole-cell, patch-clamp experiments for measuring membrane current in response to AA, $CaCl_2$ was added to the previous solution to achieve the desired free Ca^{2+} concentration (100 nM) as computed with Maxchelator. The experiments were carried out at room temperature.

Calcium Imaging

Cells were plated onto glass coverslips and were loaded with 4 μM Fura-2 AM at room temperature for 45 min in the growth medium. Recordings were performed in Maxchelator containing 140 mM NaCl, 5 mM KCl, 2 mM

$MgCl_2$, 0.3 mM Na_2HPO_3, 0.4 mM KH_2PO_4, 4 mM $NaHCO_3$, 5 mM glucose, and 10 mM HEPES adjusted to pH 7.4 with NaOH. Fluorescence images of the cells were recorded with a video image analysis system (Quanticell). In Figure 1 and Figure S1, cells were preincubated for 10 min with TG (1 μM) in Ca^{2+}-free medium to deplete ER Ca^{2+} store and then exposed to 2 mM extracellular Ca^{2+} to induce SOCE seen as $[Ca^{2+}]_c$ elevation. In Figure 3C, IM was applied to Ca^{2+}-free medium in the presence of two mitochondrial inhibitors, oligomycin (40 μM) and rotenone (20 μM).

Immunocytochemistry

Sixty percent confluent PC3 cells were washed with 1× PBS. After, PC3 cells were fixed with 4% formaldehyde-1× PBS for 15 min on ice. After three washes with 1× PBS, cells were either incubated in PBS-gelatin (PBS with 1.2% gelatin) complemented with 0.01% Tween 20 and 100 mM glycine for 30 min at 37°C. Afterward, the cells were incubated with a primary mouse monoclonal anti-ORAI1 antibody at 4°C overnight and a primary rabbit polyclonal anti-ORAI3 antibody at 37°C for 30 min. After thorough washes in PBS-gelatin, the slides were treated with the corresponding Alexa Fluor 546-labeled anti-rabbit IgG and Alexa Fluor 488-labeled anti-mouse IgG (using the dilution 1:4,000) diluted in PBS-gelatin for 1 hr at room temperature. After two washes in PBS-gelatin and one in PBS, the slides were mounted with Mowiol.

Western Blot

Protein samples (50 μg) were subjected to SDS-PAGE and transferred to a nitrocellulose membrane by semi-dry western blotting (Bio-Rad). The membrane was blocked in TNT buffer (Tris-HCl, pH 7.5, 140 mM NaCl, and 0.05% Tween 20) containing 5% milk for 45 min at room temperature. Then membranes were gently incubated overnight at 4°C with specific primary antibodies (see Supplemental Experimental Procedures). After three 5 min washes in TNT buffer, membranes were transferred into anti-rabbit IgG horseradish peroxidase-linked secondary antibodies (Chemicon, 1/50,000) or anti-mouse horseradish peroxidase-linked secondary antibodies (Chemicon, 1/10,000) for 1 hr at room temperature. After three 15 min washes in TNT buffer, the membrane was processed for chemiluminescent detection using Supersignal West Dura chemiluminescent substrate (Pierce), according to the manufacturer's instructions. A detailed method of immunoprecipitation and biotinylation of cell-surface membrane proteins is presented in Supplemental Experimental Procedures. Quantifications have been done using ImageJ software. First, each relative density of band is normalized to its standard (β-actin or calnexin) to take into account loading variation. The values present in western blot figures represent the relative density of bands compared to the control condition, which will obviously have a relative density of 1.

Animals, siRNA Injection, and Tumorigenicity Assays

Studies involving animals, including housing and care, method of euthanasia, and experimental protocols, were conducted in accordance with the local animal ethical committee in the animal house (C59-00913; protocol CEEA 202012) of the University of Sciences and Technologies of Lille, under the supervision of Dr. Lehen'kyi (59-009270). Tumor cells (2×10^6 cells/mouse) were injected subcutaneously in 50% (v:v) Matrigel (BD Biosciences) to 6- to 8-week-old male nude mice, and tumors were measured every day. When tumors grew exponentially, siRNA diluted in PBS was injected i.p. on a daily basis (120 μg/kg). Tumor volume was estimated by the following formula: length × width^2 × 0.5.

Quantitative Real-Time PCR

Quantitative real-time PCR of mRNA transcripts was done using MESA GREEN qPCR MasterMix Plus for SYBR Assay (Eurogentec) on the Bio-Rad CFX96 real-time PCR detection system. The primers used for quantitative PCR assays and siRNA sequences targeting hOrai or hSTIM1 are detailed in Supplemental Experimental Procedures.

Cell Proliferation

Cell proliferation was measured using the CellTiter 96 Aqueous One Solution cell proliferation assay (Promega). During proliferation assays, the cells were cultured in low serum condition (1% fetal calf serum).

Cell Cycle

Approximately 10^6 cells were fixed with 1 ml of ice-cold 70% methanol for 30 min. After fixing, cells were pelleted by centrifugation, washed three times with PBS at 4°C, resuspended in 100 μl of PBS, treated with 100 μl of RNase A (1 mg/ml; Sigma), and stained with propidium iodide (Sigma) at a final concentration of 50 μg/ml. The stained samples were measured on a FACScan flow cytometer (Becton-Dickinson).

Apoptosis Assay

The level of apoptosis was estimated from the number of apoptotic nuclei revealed by Hoechst staining.

SUPPLEMENTAL INFORMATION

Supplemental Information includes Supplemental Experimental Procedures and seven figures and can be found with this article online at http://dx.doi.org/10.1016/j.ccr.2014.04.025.

ACKNOWLEDGMENTS

This work was supported by grants from INSERM, la Ligue Nationale contre le Cancer, the Comité du Nord de la Ligue Nationale contre le Cancer, Université de Lille, SIRIC ONCOLille, and INCa-DGOS-Inserm 6041.

Received: January 10, 2013
Revised: March 5, 2014
Accepted: April 24, 2014
Published: June 19, 2014

REFERENCES

Berna-Erro, A., Redondo, P.C., and Rosado, J.A. (2012a). Store-operated Ca(2+) entry. Adv. Exp. Med. Biol. *740*, 349–382.

Berna-Erro, A., Galan, C., Dionisio, N., Gomez, L.J., Salido, G.M., and Rosado, J.A. (2012b). Capacitative and non-capacitative signaling complexes in human platelets. Biochim. Biophys. Acta *1823*, 1242–1251.

Brewer, J.W., and Diehl, J.A. (2000). PERK mediates cell-cycle exit during the mammalian unfolded protein response. Proc. Natl. Acad. Sci. U.S.A. *97*, 12625–12630.

Cahalan, M.D. (2009). STIMulating store-operated Ca(2+) entry. Nat. Cell Biol. *11*, 669–677.

Chen, Y.F., Chen, Y.T., Chiu, W.T., and Shen, M.R. (2013). Remodeling of calcium signaling in tumor progression. J. Biomed. Sci. *20*, 23.

Faouzi, M., Hague, F., Potier, M., Ahidouch, A., Sevestre, H., and Ouadid-Ahidouch, H. (2011). Down-regulation of Orai3 arrests cell-cycle progression and induces apoptosis in breast cancer cells but not in normal breast epithelial cells. J. Cell. Physiol. *226*, 542–551.

Feng, M., Grice, D.M., Faddy, H.M., Nguyen, N., Leitch, S., Wang, Y., Muend, S., Kenny, P.A., Sukumar, S., Roberts-Thomson, S.J., et al. (2010). Store-independent activation of Orai1 by SPCA2 in mammary tumors. Cell *143*, 84–98.

Feske, S., Gwack, Y., Prakriya, M., Srikanth, S., Puppel, S.H., Tanasa, B., Hogan, P.G., Lewis, R.S., Daly, M., and Rao, A. (2006). A mutation in Orai1 causes immune deficiency by abrogating CRAC channel function. Nature *441*, 179–185.

Flourakis, M., Lehen'kyi, V., Beck, B., Raphaël, M., Vandenberghe, M., Abeele, F.V., Roudbaraki, M., Lepage, G., Mauroy, B., Romanin, C., et al. (2010). Orai1 contributes to the establishment of an apoptosis-resistant phenotype in prostate cancer cells. Cell Death Dis. *1*, e75.

González-Cobos, J.C., Zhang, X., Zhang, W., Ruhle, B., Motiani, R.K., Schindl, R., Muik, M., Spinelli, A.M., Bisaillon, J.M., Shinde, A.V., et al. (2013). Store-independent Orai1/3 channels activated by intracrine leukotriene C4: Role in neointimal hyperplasia. Circ. Res. *112*, 1013–1025.

Hetz, C. (2012). The unfolded protein response: Controlling cell fate decisions under ER stress and beyond. Nat. Rev. Mol. Cell Biol. *13*, 89–102.

Hogan, P.G., Lewis, R.S., and Rao, A. (2010). Molecular basis of calcium signaling in lymphocytes: STIM and ORAI. Annu. Rev. Immunol. *28*, 491–533.

Holzmann, C., Kilch, T., Kappel, S., Armbrüster, A., Jung, V., Stöckle, M., Bogeski, I., Schwarz, E.C., and Peinelt, C. (2013). ICRAC controls the rapid androgen response in human primary prostate epithelial cells and is altered in prostate cancer. Oncotarget *4*, 2096–2107.

Lehen'kyi, V., Flourakis, M., Skryma, R., and Prevarskaya, N. (2007). TRPV6 channel controls prostate cancer cell proliferation via Ca(2+)/NFAT-dependent pathways. Oncogene *26*, 7380–7385.

Machaca, K. (2010). Ca(2+) signaling, genes and the cell cycle. Cell Calcium *48*, 243–250.

Magnon, C., Hall, S.J., Lin, J., Xue, X., Gerber, L., Freedland, S.J., and Frenette, P.S. (2013). Autonomic nerve development contributes to prostate cancer progression. Science *341*, 1236361.

Mercer, J.C., Dehaven, W.I., Smyth, J.T., Wedel, B., Boyles, R.R., Bird, G.S., and Putney, J.W., Jr. (2006). Large store-operated calcium selective currents due to co-expression of Orai1 or Orai2 with the intracellular calcium sensor, Stim1. J. Biol. Chem. *281*, 24979–24990.

Mignen, O., and Shuttleworth, T.J. (2000). I(ARC), a novel arachidonate-regulated, noncapacitative Ca(2+) entry channel. J. Biol. Chem. *275*, 9114–9119.

Mignen, O., Thompson, J.L., and Shuttleworth, T.J. (2008). Both Orai1 and Orai3 are essential components of the arachidonate-regulated Ca2+-selective (ARC) channels. J. Physiol. *586*, 185–195.

Mignen, O., Thompson, J.L., and Shuttleworth, T.J. (2009). The molecular architecture of the arachidonate-regulated Ca2+-selective ARC channel is a pentameric assembly of Orai1 and Orai3 subunits. J. Physiol. *587*, 4181–4197.

Monteith, G.R., McAndrew, D., Faddy, H.M., and Roberts-Thomson, S.J. (2007). Calcium and cancer: Targeting Ca2+ transport. Nat. Rev. Cancer *7*, 519–530.

Motiani, R.K., Abdullaev, I.F., and Trebak, M. (2010). A novel native store-operated calcium channel encoded by Orai3: Selective requirement of Orai3 versus Orai1 in estrogen receptor-positive versus estrogen receptor-negative breast cancer cells. J. Biol. Chem. *285*, 19173–19183.

Motiani, R.K., Zhang, X., Harmon, K.E., Keller, R.S., Matrougui, K., Bennett, J.A., and Trebak, M. (2013). Orai3 is an estrogen receptor α-regulated Ca^{2+} channel that promotes tumorigenesis. FASEB J. *27*, 63–75.

Nakanishi, M., and Rosenberg, D.W. (2006). Roles of cPLA2alpha and arachidonic acid in cancer. Biochim. Biophys. Acta *1761*, 1335–1343.

Orrenius, S., Zhivotovsky, B., and Nicotera, P. (2003). Regulation of cell death: The calcium-apoptosis link. Nat. Rev. Mol. Cell Biol. *4*, 552–565.

Patel, M.I., Kurek, C., and Dong, Q. (2008). The arachidonic acid pathway and its role in prostate cancer development and progression. J. Urol. *179*, 1668–1675.

Peinelt, C., Vig, M., Koomoa, D.L., Beck, A., Nadler, M.J., Koblan-Huberson, M., Lis, A., Fleig, A., Penner, R., and Kinet, J.P. (2006). Amplification of CRAC current by STIM1 and CRACM1 (Orai1). Nat. Cell Biol. *8*, 771–773.

Phinney, S. (1996). Metabolism of exogenous and endogenous arachidonic acid in cancer. Adv. Exp. Med. Biol. *399*, 87–94.

Prevarskaya, N., Skryma, R., and Shuba, Y. (2004). Ca2+ homeostasis in apoptotic resistance of prostate cancer cells. Biochem. Biophys. Res. Commun. *322*, 1326–1335.

Prevarskaya, N., Skryma, R., and Shuba, Y. (2011). Calcium in tumour metastasis: New roles for known actors. Nat. Rev. Cancer *11*, 609–618.

Roderick, H.L., and Cook, S.J. (2008). Ca2+ signalling checkpoints in cancer: Remodelling Ca2+ for cancer cell proliferation and survival. Nat. Rev. Cancer *8*, 361–375.

Shuttleworth, T.J. (2012). Orai3: The "exceptional" Orai? J. Physiol. *590*, 241–257.

Shuttleworth, T.J., and Thompson, J.L. (1998). Muscarinic receptor activation of arachidonate-mediated Ca2+ entry in HEK293 cells is independent of phospholipase C. J. Biol. Chem. *273*, 32636–32643.

Smyth, J.T., and Putney, J.W. (2012). Regulation of store-operated calcium entry during cell division. Biochem. Soc. Trans. *40*, 119–123.

Soboloff, J., Spassova, M.A., Tang, X.D., Hewavitharana, T., Xu, W., and Gill, D.L. (2006). Orai1 and STIM reconstitute store-operated calcium channel function. J. Biol. Chem. *281*, 20661–20665.

Thébault, S., Flourakis, M., Vanoverberghe, K., Vandermoere, F., Roudbaraki, M., Lehen'kyi, V., Slomianny, C., Beck, B., Mariot, P., Bonnal, J.L., et al. (2006). Differential role of transient receptor potential channels in Ca2+ entry and proliferation of prostate cancer epithelial cells. Cancer Res. *66*, 2038–2047.

Vanden Abeele, F., Skryma, R., Shuba, Y., Van Coppenolle, F., Slomianny, C., Roudbaraki, M., Mauroy, B., Wuytack, F., and Prevarskaya, N. (2002). Bcl-2-dependent modulation of Ca(2+) homeostasis and store-operated channels in prostate cancer cells. Cancer Cell *1*, 169–179.

Várnai, P., Hunyady, L., and Balla, T. (2009). STIM and Orai: The long-awaited constituents of store-operated calcium entry. Trends Pharmacol. Sci. *30*, 118–128.

Williams, R.T., Manji, S.S., Parker, N.J., Hancock, M.S., Van Stekelenburg, L., Eid, J.P., Senior, P.V., Kazenwadel, J.S., Shandala, T., Saint, R., et al. (2001). Identification and characterization of the STIM (stromal interaction molecule) gene family: Coding for a novel class of transmembrane proteins. Biochem. J. *357*, 673–685.

Yang, S., Zhang, J.J., and Huang, X.Y. (2009). Orai1 and STIM1 are critical for breast tumor cell migration and metastasis. Cancer Cell *15*, 124–134.

Zhang, S.L., Yeromin, A.V., Zhang, X.H., Yu, Y., Safrina, O., Penna, A., Roos, J., Stauderman, K.A., and Cahalan, M.D. (2006). Genome-wide RNAi screen of Ca(2+) influx identifies genes that regulate Ca(2+) release-activated Ca(2+) channel activity. Proc. Natl. Acad. Sci. U.S.A. *103*, 9357–9362.